

Crystal Structure of a Zinc-dependent D-Serine Dehydratase from Chicken Kidney*^[5]

Received for publication, November 6, 2010, and in revised form, May 30, 2011. Published, JBC Papers in Press, June 15, 2011, DOI 10.1074/jbc.M110.201160

Hiroyuki Tanaka^{†1}, Miki Senda^{§1}, Nagarajan Venugopalan[¶], Atsushi Yamamoto[‡], Toshiya Senda^{||2}, Tetsuo Ishida^{†3}, and Kihachiro Horiike[‡]

From the [†]Department of Biochemistry and Molecular Biology, Shiga University of Medical Science, Seta, Ohtsu, Shiga 520-2192, Japan, the [§]Structure-guided Drug Development Project, JBIC Research Institute, Japan Biological Informatics Consortium, 2-4-7 Aomi Koto-ku, Tokyo 135-0064, Japan, the [¶]National Institute of General Medical Sciences and National Cancer Institute Collaborative Access Team, Biosciences Division, Argonne National Laboratory, Argonne, Illinois 60439, and the ^{||}Biomedical Information Research Center, National Institute of Advanced Industrial Sciences and Technology, 2-4-7 Aomi Koto-ku, Tokyo 135-0064, Japan

D-Serine is a physiological co-agonist of the *N*-methyl-D-aspartate receptor. It regulates excitatory neurotransmission, which is important for higher brain functions in vertebrates. In mammalian brains, D-amino acid oxidase degrades D-serine. However, we have found recently that in chicken brains the oxidase is not expressed and instead a D-serine dehydratase degrades D-serine. The primary structure of the enzyme shows significant similarities to those of metal-activated D-threonine aldolases, which are fold-type III pyridoxal 5'-phosphate (PLP)-dependent enzymes, suggesting that it is a novel class of D-serine dehydratase. In the present study, we characterized the chicken enzyme biochemically and also by x-ray crystallography. The enzyme activity on D-serine decreased 20-fold by EDTA treatment and recovered nearly completely by the addition of Zn²⁺. None of the reaction products that would be expected from side reactions of the PLP-D-serine Schiff base were detected during the >6000 catalytic cycles of dehydration, indicating high reaction specificity. We have determined the first crystal structure of the D-serine dehydratase at 1.9 Å resolution. In the active site pocket, a zinc ion that coordinates His³⁴⁷ and Cys³⁴⁹ is located near the PLP-Lys⁴⁵ Schiff base. A theoretical model of the enzyme-D-serine complex suggested that the hydroxyl group of D-serine directly coordinates the zinc ion, and that the ε-NH₂ group of Lys⁴⁵ is a short distance from the substrate Cα atom. The α-proton abstraction from D-serine by Lys⁴⁵ and the elimination of the hydroxyl group seem to occur with the assistance of the zinc ion, resulting in the strict reaction specificity.

D-Serine is a co-agonist of the NMDA receptor, an excitatory neurotransmitter receptor important for higher brain functions, including learning and memory (1, 2). The NMDA receptor is a glutamate-gated ion channel (3), and glutamate does not activate the receptor unless a co-agonist binding site is simultaneously occupied by D-serine or glycine (4). Because significant concentrations of D-serine exist in vertebrate brains (5), D-serine is believed to physiologically control the sensitivity of the NMDA receptor to glutamate (6).

In mammals, D-serine is produced by a bifunctional serine racemase/dehydratase (7) and is mainly degraded by D-amino acid oxidase (2, 7). In rat brains, the localization of D-amino acid oxidase activity is reciprocal to that of D-serine (8, 9), suggesting that D-amino acid oxidase determines the basal levels of D-serine in mammalian brains. However, we have found recently that, in the chicken brain, D-serine is degraded mainly by a D-serine dehydratase (DSD)⁴ (10), which catalyzes the α,β-elimination of water from D-serine to form pyruvate and ammonia. In addition, we have found that the chicken DSD (chDSD) has a primary structure similar to those of metal-activated D-threonine aldolases (11–13), which are fold-type III PLP-dependent enzymes (14), and is distinct from a well known metal-independent bacterial DSD (dsdA) belonging to the fold-type II PLP-dependent enzyme family (14, 15). Interestingly, a fold-type III family protein coded by gene *YGL196W* of *Saccharomyces cerevisiae* was recently identified as a zinc-dependent DSD (scDSD) (16). To understand why avian species use DSD to metabolize D-serine in the brain and its physiological functions, it is important to reveal the structural and enzymatic properties of this novel DSD family.

In the present study, we showed that chDSD requires Zn²⁺ just as scDSD does. Then, to reveal the catalytic roles of Zn²⁺ in the dehydration of D-serine, we determined the crystal structures of chDSD, EDTA-treated chDSD, and the EDTA-treated chDSD-D-serine complex. Although there is only one DSD entry in the Protein Data Bank (PDB), DSD from *Burkholderia xenovorans* LB400 (PDB code 3GWQ), the structure contains neither PLP nor zinc, and the enzymatic properties of this DSD

* This work was supported in part by a grant-in-aid for Scientific Research from the Ministry of Education, Culture, Sports, Science, and Technology of Japan; by the New Energy and Industrial Technology Development Organization of Japan; and by a grant-in-aid (Heisei era 22) from the Shiga University of Medical Science.

The atomic coordinates and structure factors (codes 3ANU, 3AWN, and 3AWO) have been deposited in the Protein Data Bank, Research Collaboratory for Structural Bioinformatics, Rutgers University, New Brunswick, NJ (<http://www.rcsb.org/>).

^[5] The on-line version of this article (available at <http://www.jbc.org>) contains supplemental "Experimental Procedures," Tables 1 and 2, Figs. 1–7, and additional references.

¹ Both authors contributed equally to this work.

² To whom correspondence may be addressed: Biomedical Information Research Center, National Institute of Advanced Industrial Sciences and Technology, 2-4-7 Aomi Koto-ku, Tokyo 135-0064, Japan. Fax: 81-3-35998111; E-mail: toshiya-senda@aist.go.jp.

³ To whom correspondence may be addressed: Dept. of Biochemistry and Molecular Biology, Shiga University of Medical Science, Seta, Ohtsu, Shiga 520-2192, Japan. Fax: 81-77-5482157; E-mail: teishida@belle.shiga-med.ac.jp.

⁴ The abbreviations used are: DSD, D-serine dehydratase; PLP, pyridoxal 5'-phosphate; chDSD, chicken DSD; scDSD, DSD from *S. cerevisiae*; PDB, Protein Data Bank; spSR, serine racemase from *S. pombe*.

have never been reported. Therefore, the present crystal structure of chDSD is the first DSD structure known to have PLP-Lys internal aldimine, a zinc ion in the active site, and a typical fold of the fold-type III PLP-dependent enzyme family. The present crystallographic and biochemical analyses revealed that the zinc ion serves as a catalytic cofactor of chDSD to attain strict reaction specificity.

EXPERIMENTAL PROCEDURES

Enzyme Preparation—chDSD was purified from chicken kidney as described previously (11). The enzyme solution was concentrated by ultrafiltration to ~ 10 mg/ml using a YM-30 filter (Millipore, Billerica, MA). To obtain a metal-free enzyme (EDTA-treated chDSD), the concentrated solution (~ 0.5 ml) was dialyzed against 500 ml of 20 mM potassium phosphate buffer, pH 7.5, containing 5 mM EDTA, 50 μ M PLP, and 1 mM DTT, at 4 °C for 20 h. The enzyme solution was then further dialyzed twice against 500 ml of the same buffer without EDTA at 4 °C under the same conditions. The subunit and holo-subunit concentrations of chDSD were determined using the molar absorption coefficient at 280 nm of $4.64 \times 10^4 \text{ M}^{-1} \text{ cm}^{-1}$, which was estimated from the tryptophan and tyrosine contents (17), and that at 416 nm of $4.55 \times 10^3 \text{ M}^{-1} \text{ cm}^{-1}$ (11), respectively.

Enzyme Assays—chDSD activity was assayed at 37 °C by measuring the amount of pyruvate formed using the 2,4-dinitrophenylhydrazine method as described previously (11). The standard reaction mixture (200 μ l) comprised 50 mM potassium phosphate buffer, pH 7.5, 50 mM *D*-serine, and 20 μ M PLP. The reaction was started by the addition of 5 μ l of 1–5 μ M enzyme solution. To examine the effects of metal ions, the EDTA-treated enzyme was assayed using the standard reaction mixture containing various concentrations of divalent metal ions (CaCl_2 , CuCl_2 , NiSO_4 , MgCl_2 , MnCl_2 , and ZnCl_2). Kinetic analyses were performed by measuring the *D*-serine-dependent initial velocity in the presence of 0–1.0 mM *D*-2,3-diaminopropionate.

To examine the reaction specificity of chDSD for *D*-serine, we measured the amounts of 3-hydroxypyruvate, glycine, 2-aminoethanol, and *L*-serine formed under the reaction conditions in which ~ 1 μ mol of pyruvate was produced from *D*-serine. The mixture containing 50 μ l of the standard reaction mixture and 10 μ l of 20 μ M chDSD was incubated at 37 °C for 1 h. The reaction was stopped by the addition of 20 μ l of 12.5% TCA. After removing the insoluble materials by centrifugation, the concentrations of 3-hydroxypyruvate and pyruvate were determined chromatographically as described previously (10) using a 20- μ l aliquot of the supernatant. To quantify glycine, 2-aminoethanol, and *L*-serine, an aliquot of the supernatant (2 μ l) was transferred into an Eppendorf tube, 1 μ l of 1.0 mM α -amino-*n*-butyric acid was added as an internal standard and then the solution was dried under decreasing pressure. We added 40 μ l each of 0.1 M NaHCO_3 , pH 9.0, and 12.4 mM dabsyl chloride (in acetone) to the dried sample, incubated the mixture at 70 °C for 10 min, and then removed insoluble materials by centrifugation. The supernatant was dried under reducing pressure. The dried sample was dissolved with 200 μ l of 70% ethanol (in H_2O), and an aliquot (20 μ l) of the solution was applied to a Cosmosil 5C18 AR-II column (4.6 \times 150 mm; Nacalai Tesque, Kyoto, Japan). The column was developed with

25% solvent B (0–5 min) and a linear gradient from 25 to 45% solvent B (5–45 min), where solvent A was 50 mM sodium acetate, pH 4.15, and solvent B was 90% acetonitrile (in H_2O). The flow rate was 0.8 ml/min. To quantify dabsyl *L*-serine, the dabsyl serine fraction was collected, adsorbed to an Inertsil Peptides C18 column (1.0 \times 50 mm; GL Sciences, Tokyo, Japan), washed with 15% acetonitrile containing 0.1% formic acid, eluted with 80% acetonitrile containing 0.1% formic acid, and then dried under reducing pressure. The dried sample was dissolved with 40 μ l of 30 mM ammonium acetate in methanol (solvent C) and applied to a Sumichiral OA2500 column (4.6 \times 250 mm; Sumika Chemical Analysis Service, Osaka, Japan). The column was developed with solvent C at a flow rate of 1.5 ml/min.

UV-visible Spectral Studies—Absorption spectra of chDSD and EDTA-treated chDSD were recorded at pH 7.5 in 50 mM potassium phosphate buffer in the absence and presence of 18 mM *D*-serine on a UV-1800 spectrophotometer (Shimadzu, Kyoto, Japan) using a microcell with 100- μ l volume and a 1-cm light path. An aliquot of enzyme solutions (~ 20 μ l) was diluted with 500 μ l of 50 mM potassium phosphate buffer, pH 7.5, containing 1.0 μ M PLP, and reconcentrated to ~ 20 μ l using a YM-30 filter (Millipore). The base line was recorded using the filtrate. The concentrated enzyme solution was diluted to 100 μ l with the filtrate and transferred into the cell. A 10- μ l aliquot of 200-mM *D*-serine was directly added to the enzyme solution in the cell to monitor the steady-state enzyme reaction through the absorption of PLP at the active site.

Crystal Structure Determination—chDSD was crystallized by the hanging-drop vapor diffusion method (18). Briefly, the protein solution was mixed in a 1:1 ratio with reservoir solution (12–15% (w/v) PEG4000, 50 mM MES-NaOH buffer, pH 6.5, and 10% (v/v) 2-propanol) and equilibrated against 500 μ l of the reservoir solution. chDSD crystals appeared in 2–3 weeks. The crystal structure of chDSD was determined by the multiwavelength anomalous diffraction method using the crystal soaked in the artificial mother liquor (5 mM PLP, 30% (w/v) PEG4000, 100 mM MES-NaOH buffer, pH 6.5, and 10% (v/v) 2-propanol) containing 1 mM zinc acetate. The multiwavelength anomalous diffraction data were collected at BL17A at the Photon Factory (Photon Factory; KEK, Tsukuba, Japan). The wavelength for the data collections was determined from the results of an XAS measurement (Table 1). The diffraction data were processed and scaled by the program suite HKL2000 (19). The zinc positions were determined by the program SHELXD (20), and phases were calculated by the program SHARP (21). The automated model building by the program ARP/wARP (22) made an initial molecular model of 337 residues of a total of 376 residues. The remaining model was prepared manually using the program Coot (23). The crystal structure was refined at 1.9 Å resolution using the program REFMAC5 (24) in CCP4 (25) with the diffraction data collected at BL5A in Photon Factory (KEK, Japan) (Table 1). Although this crystal was not soaked in the above-described Zn^{2+} solution, a zinc ion was clearly observed between His³⁴⁷ and Cys³⁴⁹ (see footnote of Table 1). Nine residues, namely, Gly¹⁴⁰, Asn¹⁴¹, Gly¹⁸², Ala²⁹⁵–Gln²⁹⁷, and Ala³²⁶–Gly³²⁸, located in loop regions, could not be modeled due to poor electron density. The zinc site was confirmed by the dispersive difference Fourier method from a crystal that was

X-ray Structure of D-Serine Dehydratase

not soaked in the $ZnCl_2$ solution (supplemental Table 1). Because EDTA-treated chDSD did not crystallize using the reservoir solution used in chDSD crystallization, it was crystallized by the microseeding method. Microseeds were prepared by crushing the chDSD crystals. Small crystals of the EDTA-treated chDSD with a size of $\sim 0.2 \times 0.02 \times 0.01 \text{ mm}^3$ appeared in one month. Crystals of the EDTA-treated chDSD·D-serine complex were prepared by the soaking method; the crystals were soaked first in the artificial mother liquor for 15 min and then soaked in the same liquor containing 10 mM of D-serine for 60 min. Diffraction data of the EDTA-treated chDSD crystals were collected at NE3A at Photon Factory Advanced Ring (KEK) (Table 1) and were processed and scaled by the XDS program package (26). The crystal structures were determined by the difference Fourier method and refined by the program REFMAC5 (24) in CCP4 (25).

Model Building of chDSD·D-Serine Complex—The molecular model of the chDSD·D-serine complex (external aldimine intermediate) was prepared on the basis of the crystal structure of the EDTA-treated chDSD·D-serine complex. First, a zinc ion was added to the structure of the EDTA-treated chDSD, and then dihedral angles of ϕ , ψ and χ_1 of the D-serine molecule were changed so as to fulfill the Dunathan's hypothesis, *i.e.* the $C\alpha$ -H bond became nearly perpendicular to the plane of the Schiff base (27). The position of the $C\alpha$ atom of the D-serine molecule was not changed in this manual model-building step. Second, this initial model was energetically minimized using a minimization routine of the program CNS (28). Only water molecules found in the EDTA-treated chDSD·D-serine complex were included in the model.

Structural Analysis—All graphics in this manuscript were prepared by the program PyMOL. Hydrogen bonds were analyzed using the program CONTACT in CCP4 (25) with ANGH and ANGO parameters of 120 and 90, respectively.

RESULTS

Reaction Specificity—A β -hydroxy- α -amino acid-PLP Schiff base, such as a serine-PLP Schiff base, is theoretically prone to five possible reactions: α,β -elimination, transamination, retroaldol cleavage, decarboxylation, and racemization (29). To examine the reaction specificity of chDSD for D-serine, the products of the chDSD reaction were analyzed. chDSD was incubated with 50 mM D-serine at 37 °C for 1 h under reaction conditions in which about half of the substrate molecules were dehydrated into pyruvate. Neither 3-hydroxypyruvate (transamination product), glycine (retro-aldol cleavage product), 2-aminoethanol (decarboxylation product), or L-serine (racemization product) was detected (Fig. 1), whereas $\sim 1.3 \mu\text{mol}$ of pyruvate was formed. The mole ratio of the product to the enzyme subunit was 6500. Considering that the present chromatographic methods could detect each side reaction product down to a few nmol, these results suggest that no single side reaction occurred in chDSD during ~ 6000 cycles of the dehydration reaction. This high reaction specificity is a characteristic that distinguishes chDSD from bifunctional mammalian serine racemases that show physiologically significant levels of dehydratase activity (30).

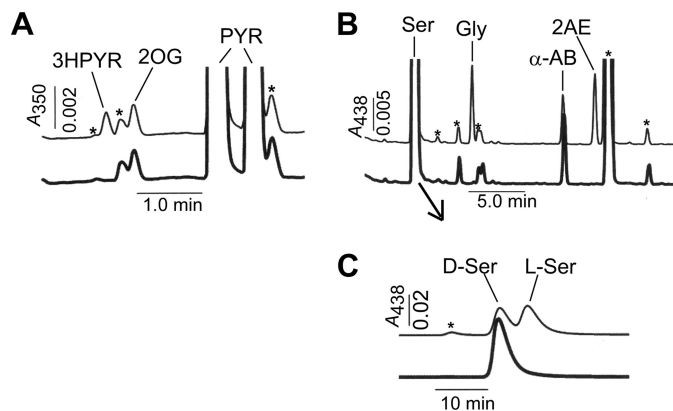


FIGURE 1. Reaction specificity of chDSD for D-serine. A, measurement of 3-hydroxypyruvate (3HPYR), a transamination product. The reaction mixture containing 2.5 μmol D-serine and 0.2 nmol chDSD was incubated at 37 °C for 1 h, and then the amounts of pyruvate (PYR) and 3-hydroxypyruvate formed were measured using 2-oxoglutarate (2OG, 2 nmol) as an internal standard. The pyruvate peaks corresponded to about 1.3 μmol . In the upper chromatogram, a known amount of 3-hydroxypyruvate (2 nmol) was added to the reaction mixture after the enzymatic reaction was stopped by the addition of TCA. B, measurement of Gly, the retro-aldol cleavage product, and 2-aminoethanol (2AE), the decarboxylation product. We added α -amino-*n*-butyric acid (α -AB, 0.5 nmol) as an internal standard to an aliquot of the TCA-stopped reaction mixture (described in A). In the upper chromatogram, known amounts of Gly and 2-aminoethanol (0.2 nmol each) were also added to the mixture. C, measurement of L-Ser, the racemization product. The serine peak (Ser) in B was collected and applied to a Sumichiral OA2500 column. In the upper chromatogram, equal amounts of dabsyl derivatives of D-Ser and L-Ser were applied to the column. The peaks labeled with asterisks in A and B were observed in the reaction mixture untreated with the enzyme.

Metal Requirement for Dehydratase Activity—scDSD, which has 31% amino acid sequence identity to chDSD, is a zinc-dependent enzyme (16). The metal dependence of chDSD was therefore examined by the addition of divalent metal ions to chDSD that was pretreated with EDTA, a procedure similar to that used for scDSD (16). The EDTA-treated chDSD retained only $\sim 5\%$ of the original catalytic activity and remained inactive even after the addition of 10 μM Zn^{2+} (Fig. 2A). However, the activity recovered rapidly up to nearly the original level as the Zn^{2+} concentration increased to 50 μM (Fig. 2A). Above 100 μM , the zinc ion showed inhibitory effects (Fig. 2A). No activation of the EDTA-treated chDSD was obtained after the addition of other divalent cations such as Mg^{2+} , Ca^{2+} , Cu^{2+} , and Ni^{2+} , whereas the addition of Mn^{2+} induced a maximal recovery of $\sim 20\%$ of the original activity in the EDTA-treated chDSD enzyme under the standard reaction mixture. The k_{cat} and K_m values of the Mn^{2+} -activated chDSD were $0.244 \pm 0.001 \text{ s}^{-1}$ and $0.34 \pm 0.13 \text{ mM}$, respectively, whereas those of the native chDSD were $2.08 \pm 0.11 \text{ s}^{-1}$ and $0.83 \pm 0.22 \text{ mM}$, respectively (supplemental Fig. 1). The k_{cat}/K_m value of Mn^{2+} -activated chDSD was 3.5-fold smaller than that of the native Zn^{2+} enzyme.

PLP-monitored Steady-state Enzyme Reaction—The absorption spectrum of chDSD showed a maximum at 412 nm (Fig. 2B, red curve). During the steady-state reaction with D-serine, a new maximum at 424 nm was observed (Fig. 2B, black curves 1–4). The absorption spectra in the 370–550 nm region did not change during the 0.5–8 min after the mixing with D-serine. The time-dependent increase in the absorption at about 320 nm is due to the increase in the concentration of pyruvate, the

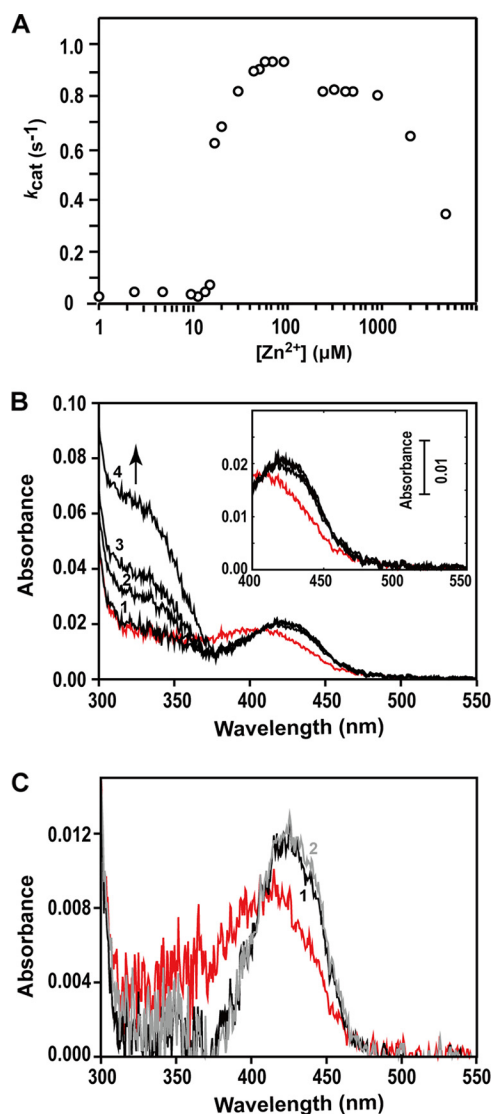


FIGURE 2. Effect of Zn^{2+} on the D-serine dehydratase activity and UV-visible absorption spectra of chDSD under steady-state reaction. A, the EDTA-treated chDSD activity was assayed using the reaction mixture (0.2 ml) containing 50 mM potassium phosphate buffer, pH 7.5, 50 mM D-serine, 20 μ M PLP, 24 pmol of the enzyme, and various concentrations of $ZnCl_2$. The k_{cat} values of the untreated and EDTA-treated chDSD were 1.0 and 0.05 s^{-1} , respectively. The activity of the EDTA-treated enzyme is unchanged in the presence of 10 μ M Zn^{2+} and recovered almost fully with the increase in the Zn^{2+} concentration from 20 to 50 μ M. This deviation from a hyperbolic curve was probably due to small amounts of EDTA retained in the EDTA-treated chDSD and rather unlikely due to cooperative binding of Zn^{2+} to the enzyme. B, absorption spectra of chDSD (holo-subunit concentration of 4.0 μ M) were recorded before (red curve) and after the addition of D-serine (black curves 1–4) were measured 0.5, 1.5, 4.0, and 8.0 min after mixing with D-serine, respectively. The inset shows enlargements of the spectra in the 400–550 nm region. C, absorption spectra of EDTA-treated chDSD (holo-subunit concentration of 2.0 μ M) were recorded before (red curve) and after the addition of D-serine (black and gray curves 1 and 2) were measured 0.5 and 20 min after mixing with D-serine, respectively.

reaction product (see the absorption spectrum of pyruvate given in supplemental Fig. 2). When the EDTA-treated enzyme was mixed with D-serine, a similar spectral change was observed (Fig. 2C) as in the case of EDTA-untreated enzyme, whereas no increase in the absorbance at 300–350 nm was observed even 20 min after the mixing with D-serine, indicating the lack of dehydratase activity. We also examined the possible nonenzymatic

reaction of enzyme-unbound PLP with D-serine. PLP reacted rapidly with D-serine to form a Schiff base, resulting in a decrease in the absorbance at 389 nm and a concomitant increase in that at 409 nm (supplemental Fig. 3A). It should be noted that no absorbance peak or shoulder was observed at either \sim 470 nm or 490 nm, the characteristic absorption peaks for the α -aminoacrylate intermediate (31), and the quinonoid intermediate (32), respectively. These results suggest that the species maximally absorbing at 424 nm is an external aldimine intermediate and that the α -proton abstraction from D-serine in the intermediate is the rate-limiting step during the steady-state course of D-serine conversion in chDSD.

Overall and Subunit Structures of chDSD—To determine the structural basis of the Zn^{2+} requirement in the catalytic reaction of chDSD, the crystal structure of chDSD was determined by the MAD method (Table 1). Although chDSD forms a dimer in solution (11), the asymmetric unit of the crystal contains one subunit. A head-to-tail dimer is formed by the crystallographic 2-fold axis with an interacting surface area of \sim 2150 \AA^2 (Fig. 3A). Considering the large interacting surface area, this crystallographic dimer is likely to correspond to the dimeric chDSD observed in solution. Of the 376 residues of the chDSD subunit, 45 residues are located in the subunit interface. The interactions between the subunits are mainly hydrophilic; there are 14 direct hydrogen bonds between the subunits. In addition to these direct interactions, 42 solvent molecules found in the subunit interface connect the subunits through their hydrogen bond networks. In the dimer, there are two symmetry-related deep pockets between the subunits. Because a PLP molecule exists at the bottom of each pocket, these pockets should be the active sites of the enzyme (Fig. 3, A and B).

The subunit consists of two domains (Fig. 3A): an N-terminal domain with an (α/β)₈ TIM-barrel fold (residues 19–246) and a C-terminal domain (residues 247–376), which also includes residues at the N terminus (residue numbers 1–18). The C-terminal domain is composed of a β -sandwich fold and five surrounding short α -helices. The overall fold of chDSD is very similar to those of prokaryotic alanine racemases (33), confirming that chDSD belongs to the PLP-dependent fold-type III enzymes.

Zinc Ion Binding Site—During chDSD model building, a strong electron density was found between His³⁴⁷ and Cys³⁴⁹. This electron density seems to represent a metal ion that coordinates the imidazole NE atom of His³⁴⁷ and the SG atom of Cys³⁴⁹ (Fig. 4A), both of which are located on helix α 15 in the C-terminal domain. A dispersive difference Fourier map, calculated with datasets collected at peak and edge wavelengths of zinc (Fig. 4A and supplemental Table 1), suggested that the strong electron density represents a zinc ion. The final model of the substrate-free form showed that the zinc ion coordinates the NE atom of His³⁴⁷ and the SG atom of Cys³⁴⁹ with coordination distances of 2.2 and 2.4 \AA , respectively. In addition to these two amino acid residues, the zinc ion coordinates three water molecules (Wat-2, Wat-3, and Wat-5) (Fig. 4A), which are connected to the active site walls through hydrogen bond networks (Fig. 4B). The zinc ion is located near the phosphate group of PLP, and is 5.2 \AA apart from the C4' atom (Fig. 4A). No other zinc

TABLE 1
Crystallographic summary

	Peak	Edge	High remote	Low remote
Structure determination (MAD data collection)^a				
Beam line		KEK Photon Factory BL17A		
Wavelength (Å)	1.2818	1.2828	1.2551	1.3030
Space group		P422		
Cell dimensions (Å)		$a = b = 104.8, c = 81.9$		
Resolution limits (Å)	50.0-2.20	50.0-2.25	50.0-2.35	50.0-2.45
Highest shell (Å)	2.28-2.20	2.33-2.25	2.43-2.35	2.54-2.45
Unique reflections	23,641 (2317) ^b	22,240 (2152)	19,683 (1893)	17,569 (1704)
Completeness (%)	99.8 (99.8)	99.8 (99.0)	99.7 (98.7)	99.8 (99.6)
Average $I/\sigma(I)$	15.7	14.9	14.4	14.3
Redundancy	7.0 (6.7)	7.0 (6.2)	7.0 (6.3)	6.9 (6.5)
R_{merge}	0.059 (0.208)	0.058 (0.264)	0.059 (0.356)	0.057 (0.448)
	Native chDSD	EDTA-treated chDSD	EDTA-treated chDSD-D-Ser	
Crystallographic refinement				
Beam line	KEK Photon Factory BL5A	KEK Photon Factory Advanced Ring NE3A	KEK Photon Factory Advanced Ring NE3A	
Wavelength (Å)	1.0000	1.0000	1.0000	
Space group	P422	P422	P422	
Cell dimensions (Å)	$a = b = 104.6, c = 81.4$	$a = b = 105.3, c = 82.0$	$a = b = 105.1, c = 81.9$	
Resolution limits (Å)	17.0-1.90	90.0-2.80	100.0-2.65	
Highest shell (Å)	2.00-1.90	2.95-2.80	2.79-2.65	
Unique reflections	35,919 (5021)	11,883 (1675)	13,850 (1924)	
Completeness (%)	99.2 (99.7)	99.9 (99.7)	99.9 (99.9)	
Average $I/\sigma(I)$	26.5 (3.5)	12.6 (3.1)	15.4 (3.5)	
Redundancy	6.9 (6.7)	6.9 (6.7)	7.0 (7.0)	
R_{merge}	0.047 (0.546)	0.155 (0.646)	0.127 (0.588)	
No. of reflections	34123	11245	13118	
$R_{\text{work}}/R_{\text{free}}$	0.189/0.215	0.211/0.257	0.206/0.266	
No. of atoms				
Protein	2778	2768	2772	
Ligand/ion	17/2	15/0	22/0	
Solvent	143	0	30	
R.m.s.d. ^c				
Bond length (Å)	0.0103	0.0105	0.0089	
Bond angle	1.309°	1.433°	1.288°	
Ramachandran plot (%)				
Most favored	88.4	85.2	84.2	
Additionally allowed	10.9	14.1	15.1	
Generously allowed	0.3	0.3	0.3	
Disallowed	0.3	0.3	0.3	

^a The crystal used for the multiwavelength anomalous diffraction data collection was soaked in Zn^{2+} -containing solution before data collection (see "Experimental Procedures"). The Zn^{2+} -soaked crystal contained two zinc ions in one subunit. Because the crystal structures of chDSD that was obtained from the crystals without soaking in the Zn^{2+} solution each contain a single zinc ion in the subunit, the second zinc ion, which is observed only in the Zn^{2+} -soaked crystal, is likely to be an artifact of the soaking.

^b Values in parentheses are for the highest resolution shell.

^c r.m.s.d., root mean square deviation.

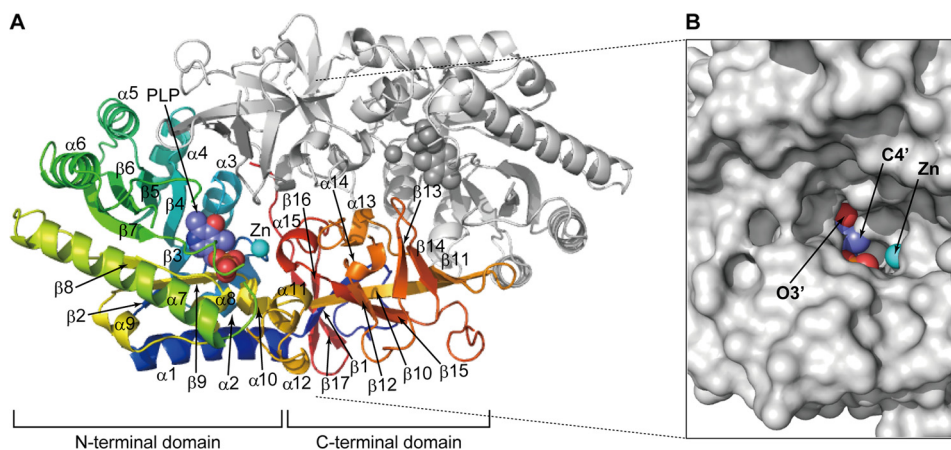


FIGURE 3. The structure of chDSD. A, dimer viewed along the crystallographic 2-fold axis. One of the subunits is shown in color (the N-terminal domain in cool colors and the C-terminal domain in warm colors), and the other subunit is shown in white. The coenzyme PLP (dark blue for carbon atoms) and zinc ion (cyan) are shown as the space-filling model. The active site pocket is formed between the two subunits. The typical α/β -barrel fold and the smaller domain composed mainly of β -strands clearly indicate that chDSD belongs to the fold-type III PLP-dependent enzyme family. B, active site pocket viewed from the solvent side. The PLP and zinc ion are shown as a space-filling model with the same color as in A. The distance between the zinc ion and the C4' atom is 5.6 Å.

ion was found in the refined crystal structure, suggesting that this zinc ion is required for the enzyme activity of chDSD.

Active Site of Substrate-Free chDSD—As described above, the active sites of chDSD are located at the dimer interface of the

enzyme and are surrounded by the C-terminal side of the TIM-barrel of the N-terminal domain, two short α -helices ($\alpha 11$ and $\alpha 15$) of the C-terminal domain, and the C-terminal domain of the adjacent subunit (helices $\alpha 13$ and $\alpha 14$, β -sheets $\beta 13$ and

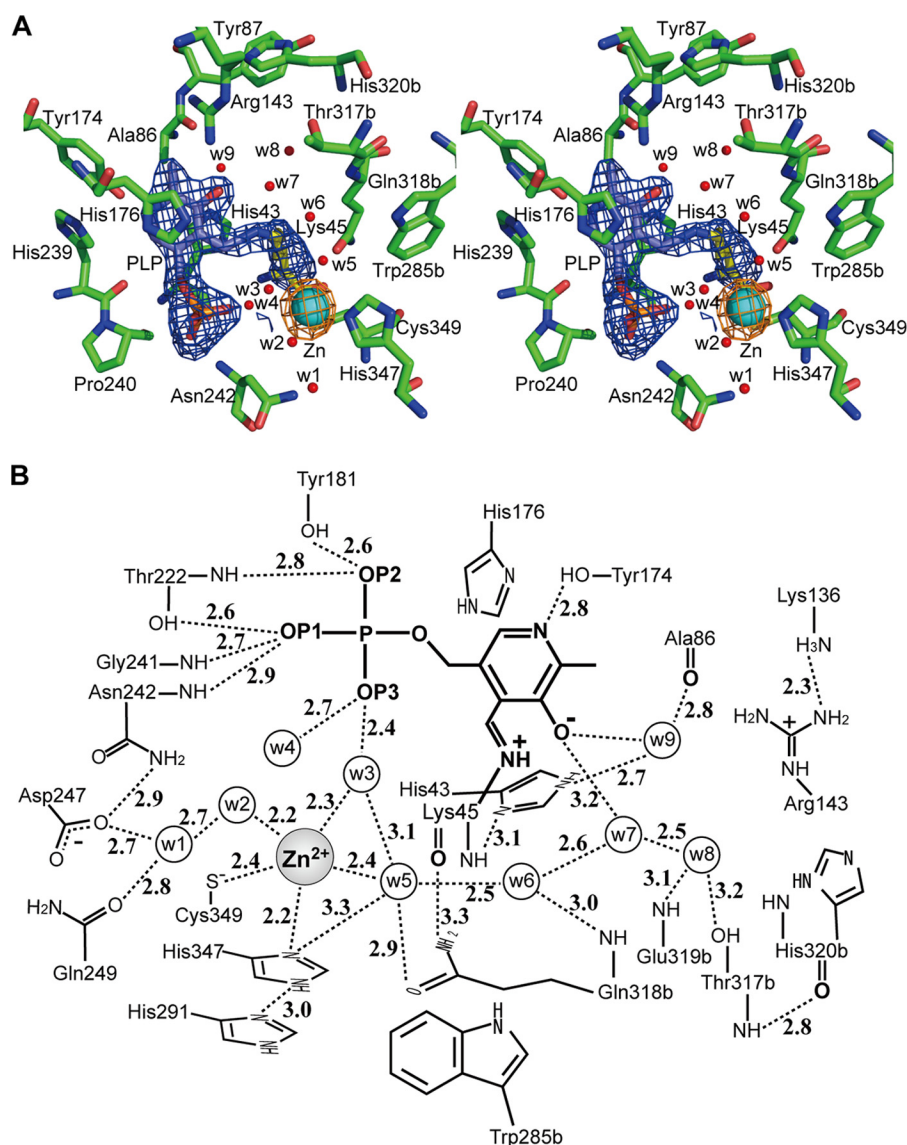


FIGURE 4. **The active site of chDSD.** A, stereoview of the active site of substrate-free chDSD. The *front* of the figure is the solvent side (entrance to the active site). The active site residues are depicted as *stick models*. The zinc ion is shown as a *cyan sphere*. A dispersive difference Fourier map ($F_{\text{peak}} - F_{\text{edge}}$) for zinc is calculated and contoured at the 5.0σ level in *orange*. An omit map for PLP contoured at the 3.0σ level in *blue* shows the PLP-Lys⁴⁵ internal Schiff base structure. Nine water molecules in the active site are shown as *red spheres*. B, a schematic diagram showing hydrogen bond, salt bridge, and zinc coordination interactions of the active site residues in substrate-free chDSD. Hydrogen bond and salt bridge interactions are depicted by *dotted lines* with the interatomic distance in Å.

β 14, and the loop between β 13 and β 14) (Fig. 3A). The active site harbors one PLP, one zinc ion, and nine water molecules (Wat-1–Wat-9, in Fig. 4, A and B).

The C4' atom of PLP forms a typical Schiff base with the NZ atom of Lys⁴⁵ (Fig. 4A). The Schiff base bond (C4' = N) is nearly coplanar with the pyridine ring of PLP (Fig. 4A). The pyridine ring is sandwiched by the imidazole rings of His⁴³ and His¹⁷⁶ from the *re*- and *si*-face sides, respectively (Fig. 4A), and the N1 atom forms a hydrogen bond with the phenolic hydroxyl group of Tyr¹⁷⁴ (Fig. 4, A and B). Because the N1 atom is likely to act as an acceptor of this hydrogen bond, the N1 atom is likely to be deprotonated. The phosphate group of PLP interacts with main chain N atoms of Thr²²², Gly²⁴¹, Asn²⁴², and the hydroxyl groups of Tyr¹⁸¹ and Thr²²² (Fig. 4B). Two water molecules (Wat-3 and Wat-4) form hydrogen bonds with the OP3 atom of the phosphate group (Fig. 4B), and one of the water molecules

(Wat-3) is coordinated by the zinc ion. The O3' atom of PLP forms a hydrogen bond with a water molecule (Wat-9), which, in turn, forms hydrogen bonds with the imidazole NE atom of His⁴³ and the main chain O atom of Ala⁸⁶ (Fig. 4B).

Crystal Structure of EDTA-treated chDSD—Biochemical studies showed that the zinc ion is required for the enzyme activity of chDSD (Fig. 2A). Some PLP-dependent enzymes also require a metal ion for their enzyme activities. However, unlike chDSD, these enzymes have the activity-relevant metal ion outside of their active site, thus it is proposed that these metal ions are essential to stabilize the catalytically competent conformation of the enzyme (structural cofactors) and are not directly involved in the catalytic reaction (34, 35). To investigate whether the zinc ion is required to maintain the structure of catalytically competent chDSD, we determined the crystal structure of the EDTA-treated chDSD (Table 1). As expected,

X-ray Structure of D-Serine Dehydratase

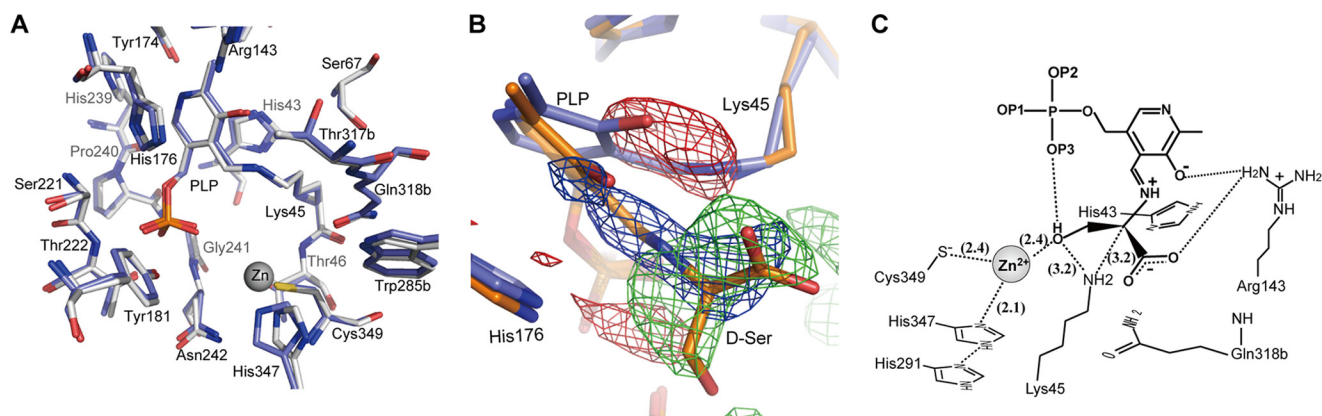


FIGURE 5. The active site of EDTA-treated chDSD and its complex with D-serine. *A*, superposition of the active site of EDTA-treated chDSD (carbon atoms in blue) and chDSD (carbon atoms in white). The gray sphere is a zinc ion observed only in chDSD. *B*, the $F_{o(D-SER)} - F_{o(FREE)}$ difference Fourier map of the EDTA-treated chDSD. $F_{o(D-SER)}$ and $F_{o(FREE)}$ represent observed structure factors from EDTA-treated chDSD crystals soaked in the artificial mother liquor with and without 10 mM of D-serine, respectively. The maps were contoured at the $+3.5\sigma$ level (blue) and the -3.5σ level (red). The omit map for the D-serine molecule is also shown, which is contoured at the 3.0σ level (green). Although both of the internal and external aldimines are observed in the crystal structure of the EDTA-treated chDSD-D-serine complex, only the external aldimine is depicted in the figure for clarity. Carbon atoms of EDTA-treated chDSD and its D-serine complex are shown in blue and orange, respectively. *C*, schematic diagram of the energy-minimized model of the chDSD-D-serine complex (an external aldimine intermediate) built on the basis of the active site of the EDTA-treated chDSD-D-serine complex. Predicted hydrogen bonds are shown by dotted lines. Values in parentheses are distances between two atoms found in the energy minimized model structure.

the crystal structure of the EDTA-treated chDSD showed no electron densities for the zinc ion in the active site (supplemental Fig. 4). Importantly, no significant conformational changes were observed in the structure of chDSD before and after the EDTA treatment; Lys⁴⁵ and PLP formed a Schiff base in both structures, and overall, the root mean square deviation of the C α atoms was 0.24 Å. With the exception of His³⁴⁷, none of the residues in the active sites showed significant conformational changes (Fig. 5A). The χ_2 angle of His³⁴⁷ rotates by $\sim 40^\circ$, probably due to the loss of the coordination to the zinc ion. This result suggested that the zinc ion is unlikely to be a structural cofactor.

Crystal Structure of EDTA-treated chDSD in Complex with D-Serine—Because chDSD retains the original conformation of the active site without the zinc ion, it was expected that D-serine could bind to the EDTA-treated chDSD. In fact, when the EDTA-treated chDSD was mixed with D-serine, a shift in the absorbance maximum from 415 to 426 nm was observed (Fig. 2C), which suggested the formation of an external aldimine intermediate. To confirm this, we soaked a crystal of the EDTA-treated chDSD in the mother liquor containing D-serine and determined its crystal structure (Table 1). An $F_{o(D-SER)} - F_{o(FREE)}$ difference Fourier map between the EDTA-treated chDSD with and without soaking in the D-serine-containing solution revealed that D-serine forms a Schiff base with PLP in the active site (Fig. 5B). It must be noted that a part of chDSD molecule in the crystal remained in the internal aldimine state, in which Lys⁴⁵ forms a Schiff base with PLP. In the EDTA-treated chDSD-D-serine complex, the carboxyl group of the D-serine interacts with the main chain N atom of Gln³¹⁸ of the other subunit (3.3 Å), and the C α -H bond of the D-serine is nearly parallel to the Schiff base/pyridine ring plane and not perpendicular to the plane.

Interestingly, the binding of D-serine to the active site induced a rotation of the pyridine ring of PLP by $\sim 35^\circ$ (Fig. 5B). A similar rotation of the pyridine ring was observed in the crystal structure of the chDSD-D-2,3-diaminopropionate complex

(supplemental Fig. 5). These results suggest that the breakage of the Schiff base bond between Lys⁴⁵ and PLP induces the rotation of the pyridine ring of PLP, resulting in an interaction between the NH₂ group of Arg¹⁴³ and the O3' atom of PLP (3.0 Å).

Structural Model of chDSD-D-Serine Complex—To examine the substrate recognition and the reaction mechanism, we built a model of the external aldimine form of the chDSD-D-serine complex on the basis of the crystal structure of the EDTA-treated chDSD-D-serine complex (Fig. 5C). By rotating only the ϕ dihedral angle of the bound D-serine molecule, we could align the C α -H bond perpendicular to the coenzyme planar π -bonding system, consistent with α -proton elimination according to the Dunathan's hypothesis (27, 29). Then, the χ dihedral angle of the D-serine was rotated to allow its hydroxyl group to interact with the zinc ion. Thirdly, we rotated the ψ dihedral angle of the D-serine so that its carboxyl group formed a hydrogen bond with the NH₂ group of Arg¹⁴³. Finally, the model structure was subjected to energy minimization. In the refined model (Fig. 5C), the side chain of Lys⁴⁵ is located in the *re*-face side of PLP, and the NZ atom of Lys⁴⁵ is located at a distance of ~ 3.2 Å from the C α and hydroxyl O atoms of D-serine. It is of note that the NZ atom of Lys⁴⁵ can further approach the C α and hydroxyl O atoms of D-serine (< 3 Å) when rotation of the dihedral angles is allowed for the side chain of Lys⁴⁵.

Structural Comparison with Related Proteins—A structural homology search using the DALI server (36) showed that there are several structural homologues of chDSD in PDB. Most of them are functionally known proteins such as amino acid racemases and decarboxylases. The protein with a structure most similar to that of chDSD was a zinc ion- and PLP-containing protein, which is derived from *Idiomarina loihiensis* L2TR (YP_156143.1) (PDB code 3LLX). The crystal structure of PDB code 3LLX was determined in a structural genomics project (Joint Center for Structural Genomics) (37). The function of the protein remains unknown. The structural alignment with 3LLX using 354 residues gave a Z-score of 45.2 and a root mean

DISCUSSION

Zinc Ion in Active Site—The dispersive anomalous difference Fourier map revealed unambiguously that chDSD has one zinc ion in the active site (Fig. 4A). Because no zinc ions were added in the buffers used for the purification and crystallization of the enzyme, chDSD seems to contain the zinc ion under physiological conditions, although manganese ions can partially restore the enzyme activity.

The coordination sphere of the zinc ion has a unique character: only two protein residues, His³⁴⁷ and Cys³⁴⁹, are coordinated to the zinc ion together with three solvent molecules (Fig. 4B). Our comprehensive analysis of zinc centers in the proteins deposited in the PDB revealed that two-protein residue coordination is relatively unusual, found in only ~10% of all of the zinc-coordination spheres in the proteins examined (supplemental Fig. 6). Furthermore, to the best of our knowledge, with the exception of artificially engineered enzymes, this is the first example of a catalytic zinc ion coordinated by only two protein residues (see below). In typical catalytic zinc centers, the zinc ion is coordinated by three protein residues (38).

The Zn–N (His³⁴⁷) and Zn–S (Cys³⁴⁹) bond lengths in chDSD are within the respective average values of zinc-containing proteins so far determined (supplemental Fig. 7). The binding of the zinc ion with only two protein residues seems to be relatively weak, in which case the enzyme might easily lose the zinc ion. However, an intensive EDTA treatment was needed to inactivate the enzyme. In addition, crystallographic analysis suggested that the zinc ion occupancy in the active site was ~0.5 even after purification and crystallization without external addition of zinc ions. The intensive hydrogen bond network involving three water molecules that coordinate the zinc ion seems to strengthen the binding of zinc ion. These water molecules are connected to the residues lining the surface of the active site pocket (Fig. 4B). In the case of 3LLX, whose enzymatic activity is still uncertain, two protein residues and one Tris molecule are coordinated to the zinc ion: the NE2 atom of His³⁴⁶, the SG atom of Cys³⁴⁸, and the nitrogen atom and two oxygen atoms of the Tris molecule comprise the coordination sphere.

Catalytic Role of Zinc in chDSD—The present study showed that chicken DSD requires Zn²⁺ for its activity, as observed in scDSD (16). The requirement of a metal ion for the enzyme activity is prevalent among PLP-dependent enzymes. Because in all the atomic resolution structures reported hitherto a metal ion is found outside of the active site and this ion has been considered to act as a structural cofactor that stabilizes the catalytically competent conformation of the respective enzymes (34, 35). However, the present biochemical and crystallographic analyses strongly suggest that the zinc ion in chDSD is directly involved in the catalytic reaction; a zinc ion is located in the active site and can coordinate the hydroxyl group of the substrate during the catalytic reaction (Fig. 5C). Indeed, the active site structure of chDSD did not change after the zinc ion was removed by the EDTA treatment (Fig. 5A), indicating that the zinc ion does not play a role as a structural cofactor in chDSD. In fact, D-serine can form a Schiff base with PLP without a zinc ion in the active site, as revealed in the spectroscopic

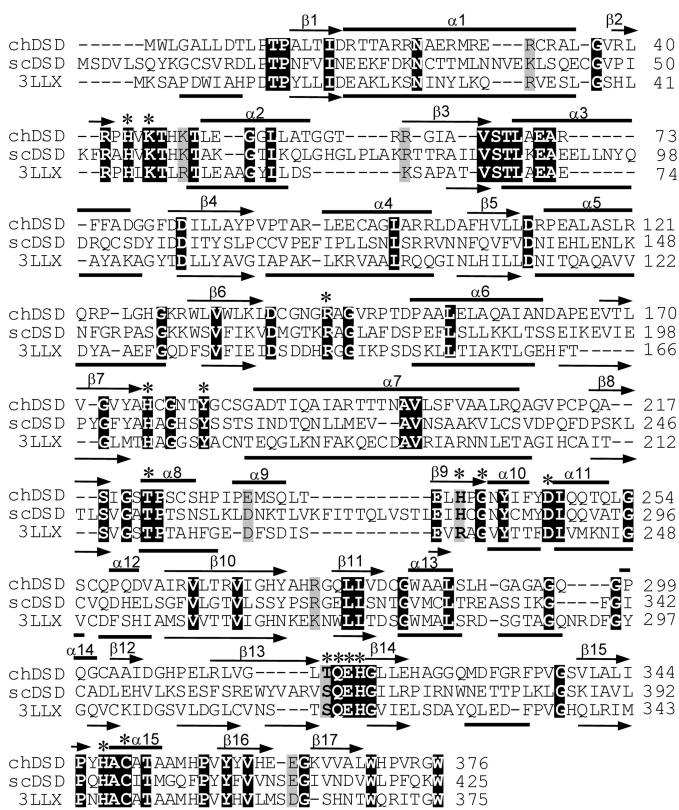


FIGURE 6. Alignment of the amino acid sequences of chDSD, scDSD, and a functionally unknown protein (3LLX) from *I. loihiensis* L2TR. The amino acid sequences are aligned on the basis of the crystal structure of chDSD. The secondary structures of chDSD and 3LLX (PDB code 3LLX) are shown by the arrow (β -sheet) and bar (α -helix). The 15 residues labeled with asterisks are those found in the active site of chDSD. Residues identical among the three sequences are shown in white letters.

square deviation of 1.9 Å for C α atoms. Of the 354 amino acid residues, 32% were identical to chDSD.

Considering the crystal packing and the structural similarity to chDSD, 3LLX seems to be a dimeric protein, whose 2-fold axis is coincident with a crystallographic 2-fold axis; two monomers of 3LLX are aligned in a head-to-tail manner. As observed in chDSD, the subunit interactions are mainly electrostatic with 24 direct hydrogen bonds between them. In 3LLX, two large pockets are found in the putative subunit interface, and each of the pockets contains one PLP molecule, which forms a Schiff base with Lys⁴⁶, and one zinc ion. The amino acid sequence alignment of chDSD, scDSD, and 3LLX on the basis of the present crystal structure (Fig. 6) showed that all the active site residues except Tyr¹⁷⁴ are conserved among them. (The 15 residues are indicated with asterisks in Fig. 6.) In chDSD, Tyr¹⁷⁴ forms a hydrogen bond with the N1 atom of PLP; the N1 atom of PLP in 3LLX forms a hydrogen bond with the side chain of Arg²³³. The superposition of the crystal structures of chDSD and 3LLX showed that the spatial organization of PLP, the zinc ion, and the conserved amino acid residues in 3LLX is nearly identical to that in chDSD. These results suggest that protein 3LLX from *I. loihiensis* has D-serine dehydratase activity, although 3LLX has been predicted to be a racemase or amino acid aldolase.

X-ray Structure of D-Serine Dehydratase

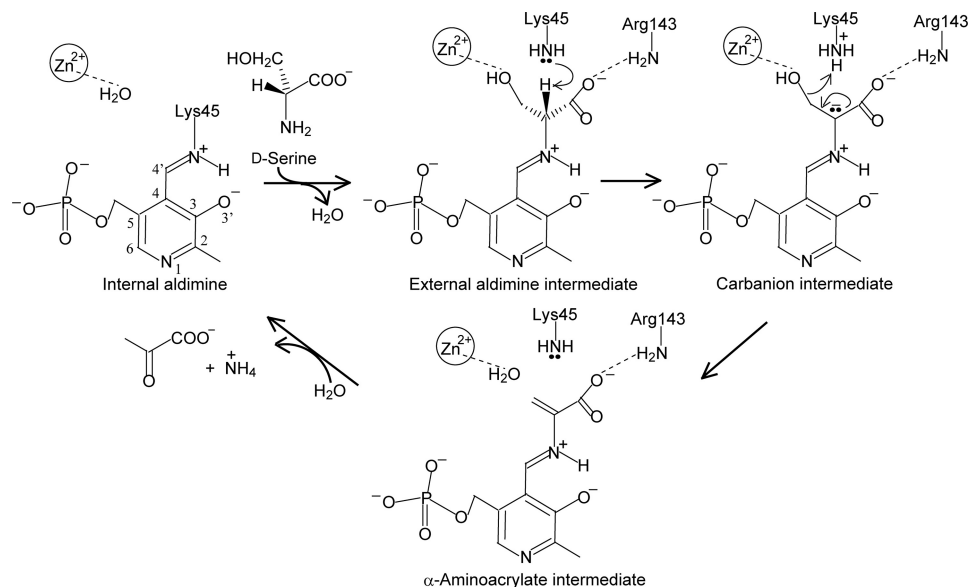


FIGURE 7. Zinc-involving reaction mechanism of chDSD with the substrate D-serine. α -Aminoacrylate is nonenzymatically hydrolyzed into pyruvate and an ammonium ion.

analyses and the crystal structure of the EDTA-treated chDSD·D-serine complex (Fig. 2, B and C, and Fig. 5B), probably suggesting that the zinc ion is essential for the reaction step(s) after the formation of the external aldimine intermediate. The theoretical model of the external aldimine intermediate (Fig. 5C) suggested that the interaction between the zinc ion and the β -hydroxyl group of the D-serine finely tunes the orientation of the C α -H bond to be scissile against the plane of the Schiff base π electron system (27).

On the basis of these experimental results, the following reaction mechanism can be proposed (Fig. 7). Initially, D-serine enters the active site pocket and approaches the *si*-face side of the Schiff base of PLP-Lys⁴⁵ (internal aldimine). The unprotonated α -amino group of the substrate makes a nucleophilic attack on the C4' atom of the internal aldimine to form an external aldimine intermediate (Fig. 7), and the side chain of Lys⁴⁵ is released in the neutral form. One of the water molecules in the active site (Wat-1–Wat-5) may deprotonate the α -amino group of the substrate. During this conversion from the internal aldimine to the external aldimine, a rotation of the pyridine ring of PLP occurs (Fig. 5B and supplemental Fig. 5). This rotation and the interaction between the zinc ion and β -hydroxyl group of D-serine seem to be important for bringing the C α -H bond nearly perpendicular to the Schiff base/pyridine ring plane. The next step seems to be an α -proton elimination of the substrate. Judging from the PLP·D-serine external aldimine model (Fig. 5C and Fig. 8A), Lys⁴⁵ directs its side chain amino group toward the α -proton of the substrate. The amino group of Lys⁴⁵ eliminates the C α proton, forming a carbanion intermediate (Fig. 7). Considering that the NZ atom of Lys⁴⁵ can approach the hydroxyl O atom of the substrate at a distance <3 Å in the external aldimine intermediate, the protonated Lys⁴⁵ can donate a proton to the substrate hydroxyl group to facilitate the β -elimination reaction, producing the PLP- α -aminoacrylate Schiff base and a water molecule. The zinc ion might facilitate the elimination of the hydroxyl group by stabilizing electrostatically the developing negative charge on the leaving hydroxyl group.

The chDSD is the first example of a PLP-dependent enzyme that possesses a metal ion as a catalytic cofactor in the active site. Considering the structural similarity and/or zinc dependence of the enzyme, scDSD and 3LLX are likely to belong to the same enzyme subfamily as chDSD (Fig. 6). Our biochemical analysis showed that chDSD can use not only Zn²⁺ but also Mn²⁺ for the catalytic reaction, the latter ion being able to coordinate N and S atoms. Interestingly, D-threonine aldolases, which belong to fold-type III PLP-dependent enzymes, preserve the same metal-binding motif of His-X-Cys/Asp in the C-terminal region as found in chDSD and require an Mn²⁺ ion for the α -elimination of D-threonine to produce acetaldehyde and glycine (12). Although the crystal structure of D-threonine aldolases has not been solved, the present crystal structure of chDSD suggests that the hydroxyl group of the substrate perpendicular to the PLP π -bonding system in the external aldimine intermediate and also to reduce the pK_a value of the substrate hydroxyl group, which is attacked by a catalytic base.

Mechanistic Implications in dsdA—Biochemical studies of D-serine dehydratase from *Escherichia coli* (dsdA) has long been available in the literature (39, 40), although its crystal structure remains elusive. dsdA is a monomeric enzyme whose primary structure shows no homology with chDSD (39). In addition dsdA has a characteristic glycine-rich region, which is suggested to control the orientation of PLP in the active site through direct interaction (39). However, no glycine-rich region is found in the primary structure of chDSD. In chDSD, two glycine residues (Gly²²⁰ and Gly²⁴¹) interact with PLP, but they do not control the orientation of PLP in chDSD. This suggests that dsdA and chDSD have distinct structural characteristics.

In the case of dsdA, a transient intermediate with a distinctive absorption peak ~ 455 nm was observed during the steady-state reaction with D-serine, and this intermediate was proposed to be the Schiff base of α -aminoacrylate and PLP (40). However, in the case of chDSD, an intermediate with an

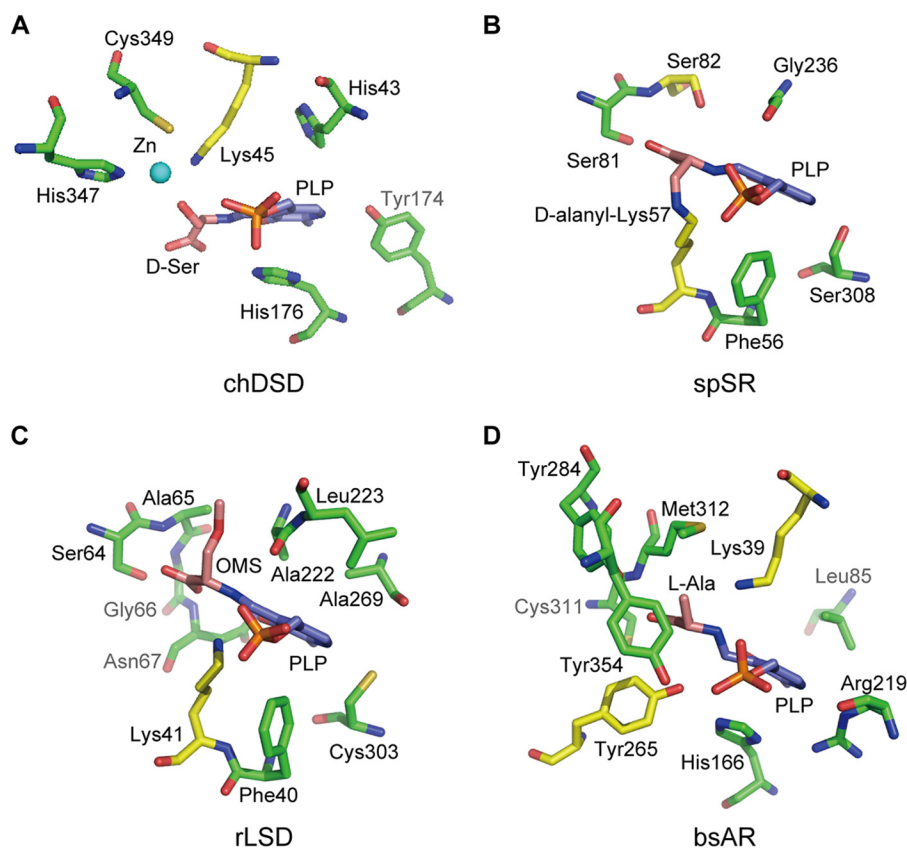


FIGURE 8. Comparison of the external aldimine structures of D-serine-bound chDSD (A) with those of L-serine-bound modified serine racemase from *S. pombe* (spSR) (B), O-methylserine-bound rat L-serine dehydratase (rLSD; C), and L-alanine-bound alanine racemase from *B. stearothermophilus* (D). Carbon atoms of catalytic bases are shown in yellow with the nitrogen atom and the oxygen atom in blue and red, respectively. Carbon atoms in cofactor PLP are shown in blue. The Lys⁵⁷ in spSR is converted to lysine-D-alanyl residue, and the amino group of D-alanyl moiety forms a Schiff base with PLP (34). The PDB codes of spSR, rat L-serine dehydratase (rLSD), and alanine racemase from *Bacillus stearothermophilus* (bsAR) are 2ZR8, 1PWH, and 1L6F, respectively.

absorption peak at 424 nm was observed during the steady-state reaction with D-serine (Fig. 2, B and C), which seems to be an external aldimine intermediate, not the α -aminoacrylate intermediate.

The present crystal structures suggest that the α -aminoacrylate intermediate proposed for dsdA can be accommodated in the active site of chDSD, and the carboxyl group of the α -aminoacrylate seems to interact with Arg¹⁴³ (Fig. 7). Single-turnover studies of chDSD and a crystallographic study of dsdA, along with a comparative analysis of the results, will be important to understand the convergent evolution of these two enzymes.

Structural Basis of Reaction Specificity—chDSD shows no detectable levels of serine racemase activity, whereas serine racemases from mammals and *Schizosaccharomyces pombe* (spSR) show significant serine dehydratase activity (30, 34). To understand the structural basis of the lack of racemase activity of chDSD, we compared the active site structures of chDSD and spSR. The configurations of the NZ atom of Lys⁴⁵, the C β atom of D-serine, and the OP3 atom of the phosphate group of PLP in chDSD are strikingly similar to those of the OG atom of Ser⁸², the C β atom of the D-alanyl moiety of the modified Lys⁵⁷, and the OP1 atom of PLP in spSR, respectively (Fig. 8, A and B). Interestingly, in rat L-serine dehydratase (35), the NZ atom of Lys⁴¹, the C β atom of O-methylserine, and the OP2 atom of PLP are arranged in a nearly mirror image of the above-de-

scribed configuration in chDSD and spSR (Fig. 8C), probably due to the difference in substrate chirality. These results suggest that in the external aldimine intermediate, dehydration can occur when (i) one catalytic acid/base exists near the C α atom and (ii) the hydroxyl group of the substrate forms a hydrogen bond with one of the oxygen atoms of the phosphate group of PLP. On the other hand, it has been established that racemases require a pair of acid/base residues as observed in the alanine racemase from *Bacillus stearothermophilus* (Lys³⁹ and Tyr²⁶⁵ in Fig. 8D) (41). The lack of the second base in chDSD explains the fact that chDSD does not have racemase activity.

The absence of the transamination activity in chDSD can also be explained on the basis of the present crystal structure. In the case of aminotransferases, an acidic residue forms a hydrogen bond with the N1 atom, resulting in the protonation of the N1 atom (42). Importantly, the quinonoid intermediate, which is necessary for conversion to the ketimine intermediate in the transamination reaction (42), is stabilized through the protonated N1 atom. On the other hand, because the N1 atom of PLP forms a hydrogen bond with the hydroxyl group of Tyr¹⁷⁴ in chDSD (Fig. 4B), the N1 atom is highly likely to behave as a proton acceptor in the hydrogen bond. Therefore, the quinonoid intermediate cannot be stabilized in the active site of chDSD. The presence of Tyr¹⁷⁴ within the hydrogen bond length seems to prevent the transamination in chDSD. It is noteworthy that the N1 atom of PLP forms a hydrogen bond

X-ray Structure of D-Serine Dehydratase

with the side chain of Tyr, Cys, Ser, or Arg in the structures shown in Fig. 8. Considering the pK_a values of the N1 atom of PLP and of the counterpart residues for the hydrogen bond, these N1 atoms are unlikely to be protonated, suggesting that none of the enzymes shown in Fig. 8 have transamination activity.

In summary, we have determined the crystal structures of chDSD, a member of a newly found PLP-dependent enzyme family that requires a zinc ion. Although a Mn^{2+} ion can partially replace the catalytic role of the zinc ion, the natural metal ion of chDSD seems to be zinc. The zinc ion is located in the active site near the coenzyme PLP and is involved in the catalytic reaction. This is the first report of a catalytic zinc ion in a PLP-dependent enzyme. Based on these structures, we have proposed a novel reaction mechanism in which the zinc ion coordinates the substrate hydroxyl group and facilitates β -elimination.

REFERENCES

- Schell, M. J. (2004) *Philos. Trans. R. Soc. Lond. B Biol. Sci.* **359**, 943–964
- Verrall, L., Burnet, P. W., Betts, J. F., and Harrison, P. J. (2010) *Mol. Psychiatry* **15**, 122–137
- Paoletti, P., and Neyton, J. (2007) *Curr. Opin. Pharmacol.* **7**, 39–47
- Wolosker, H., Dumin, E., Balan, L., and Foltyn, V. N. (2008) *FEBS J.* **275**, 3514–3526
- Hashimoto, A., and Oka, T. (1997) *Prog. Neurobiol.* **52**, 325–353
- Oliet, S. H., and Mothet, J. P. (2009) *Neuroscience* **158**, 275–283
- Pollegioni, L., and Sacchi, S. (2010) *Cell. Mol. Life Sci.* **67**, 2387–2404
- Horiike, K., Tojo, H., Arai, R., Nozaki, M., and Maeda, T. (1994) *Brain Res.* **652**, 297–303
- Nagata, Y., Horiike, K., and Maeda, T. (1994) *Brain Res.* **634**, 291–295
- Tanaka, H., Yamamoto, A., Ishida, T., and Horiike, K. (2007) *Anal. Biochem.* **362**, 83–88
- Tanaka, H., Yamamoto, A., Ishida, T., and Horiike, K. (2008) *J. Biochem.* **143**, 49–57
- Liu, J. Q., Dairi, T., Itoh, N., Kataoka, M., Shimizu, S., and Yamada, H. (1998) *J. Biol. Chem.* **273**, 16678–16685
- Paiardini, A., Contestabile, R., D'Aguanno, S., Pascarella, S., and Bossa, F. (2003) *Biochim. Biophys. Acta* **1647**, 214–219
- Grishin, N. V., Phillips, M. A., and Goldsmith, E. J. (1995) *Protein Sci.* **4**, 1291–1304
- Federiuk, C. S., Bayer, R., and Shafer, J. A. (1983) *J. Biol. Chem.* **258**, 5379–5385
- Ito, T., Hemmi, H., Kataoka, K., Mukai, Y., and Yoshimura, T. (2008) *Biochem. J.* **409**, 399–406
- Pace, C. N., Vajdos, F., Fee, L., Grimsley, G., and Gray, T. (1995) *Protein Sci.* **4**, 2411–2423
- Senda, M., Tanaka, H., Ishida, T., Horiike, K., and Senda, T. (2011) *Acta Crystallogr. Sect. F Struct. Biol. Cryst. Commun.* **67**, 147–149
- Otwinowski, Z., and Minor, W. (1997) *Methods Enzymol.* **276**, 307–326
- Schneider, T. R., and Sheldrick, G. M. (2002) *Acta Crystallogr. D.* **58**, 1772–1779
- Bricogne, G., Vonrhein, C., Flensburg, C., Schiltz, M., and Paciorek, W. (2003) *Acta Crystallogr. D.* **59**, 2023–2030
- Perrakis, A., Morris, R., and Lamzin, V. S. (1999) *Nature Struct. Biol.* **6**, 458–463
- Emsley, P., Lohkamp, B., Scott, W. G., and Cowtan, K. (2010) *Acta Crystallogr. D* **66**, 486–501
- Murshudov G. N., Vagin, A. A., and Dodson, E. J. (1997) *Acta Crystallogr. D.* **53**, 240–255
- Collaborative computational project number 4 (1994) *Acta Crystallogr. D.* **50**, 760–763
- Kabsch, W. (1993) *J. Appl. Cryst.* **26**, 795–800
- Dunathan, H. C. (1966) *Proc. Natl. Acad. Sci. U.S.A.* **55**, 712–716
- Brünger, A. T., Adams, P. D., Clore, G. M., DeLano, W. L., Gros, P., Grosse-Kunstleve, R. W., Jiang, J. S., Kuszewski, J., Nilges, M., Pannu, N. S., Read, R. J., Rice, L. M., Simonson, T., and Warren, G. L. (1998) *Acta Crystallogr. D.* **54**, 905–921
- Toney, M. D. (2005) *Arch. Biochem. Biophys.* **433**, 279–287
- Foltyn, V. N., Bendikov, I., De Miranda, J., Panizzutti, R., Dumin, E., Shleper, M., Li, P., Toney, M. D., Kartvelishvili, E., and Wolosker, H. (2005) *J. Biol. Chem.* **280**, 1754–1763
- Koutmos, M., Kabil, O., Smith, J. L., and Banerjee, R. (2010) *Proc. Natl. Acad. Sci. U.S.A.* **107**, 20958–20963
- Ikushiro, H., Fujii, S., Shiraiwa, Y., and Hayashi, H. (2008) *J. Biol. Chem.* **283**, 7542–7553
- Couñago, R. M., Davlieva, M., Strych, U., Hill, R. E., and Krause, K. L. (2009) *BMC Struct. Biol.* **9**, 53
- Goto, M., Yamauchi, T., Kamiya, N., Miyahara, I., Yoshimura, T., Mihara, H., Kurihara, T., Hirotsu, K., and Esaki, N. (2009) *J. Biol. Chem.* **284**, 25944–25952
- Yamada, T., Komoto, J., Takata, Y., Ogawa, H., Pitot, H. C., and Takusagawa, F. (2003) *Biochemistry* **42**, 12854–12865
- Holm, L., and Sander, C. (1996) *Science* **273**, 595–603
- Stevens, R. C., Yokoyama, S., and Wilson, I. A. (2001) *Science* **294**, 89–92
- Vallee, B. L., and Auld, D. S. (1990) *Proc. Natl. Acad. Sci. U.S.A.* **87**, 220–224
- Marceau, M., McFall, E., Lewis, S. D., and Shafer, J. A. (1988) *J. Biol. Chem.* **263**, 16926–16933
- Schnackerz, K. D., Ehrlich, J. H., Giesemann, W., and Reed, T. A. (1979) *Biochemistry* **18**, 3557–3563
- Watanabe, A., Yoshimura, T., Mikami, B., Hayashi, H., Kagamiyama, H., and Esaki, N. (2002) *J. Biol. Chem.* **277**, 19166–19172
- Hayashi, H. (1995) *J. Biochem.* **118**, 463–473